Chin. Sci. Bull.
DOI 10.1007/s11434-014-0643-5

csb.scichina.com
www.springer.com/scp

Review

Materials Science

Selected multiferroic perovskite oxides containing rare earth and transition metal elements

Shunbo Hu · Lei Chen · Yabei Wu · Liming Yu · Xinluo Zhao · Shixun Cao · Jincang Zhang · Wei Ren

Received: 21 May 2014 / Accepted: 28 July 2014

Abstract Multiferroic materials are currently the subject of intensive research worldwide, because of both their fundamental scientific problems and also possible technological applications. Among a number of candidates in the laboratories, compounds consisting of rare earth and transition metal perovskite oxides have very unusual structural and physical properties. In contrast to the so-called type I multiferroics, ferroelectricity may be induced by magnetic ordering or by applying external fields. In this review, the recent progress on the experimental and theoretical studies of some selected type II multiferroics is presented, with a focus on the perovskite oxides containing rare earth and transition metal elements. The rare earth orthoferrite crystals, rare earth titanate strained film, and rare earth-based superlattices are systematically reviewed to provide a broad overview on their promising electric, magnetic, and structural properties. The recent experimental advances in single-crystal growth by optical floating zone method are also presented. First-principles investigations, either supported by experimental results or awaiting for experimental verifications, are shown to offer useful guidance for the future applications of unconventional multiferroics.

Keywords Multiferroics · Rare earth · Transition metal · Perovskite · Epitaxial strain · Superlattice

SPECIAL TOPIC: Multiferroic Materials

S. Hu · L. Chen · Y. Wu · L. Yu · X. Zhao · S. Cao · J. Zhang · W. Ren (✉)
Department of Physics, Shanghai University, Shanghai 200444, China
e-mail: renwei@shu.edu.cn

1 Introduction

The combination of (anti)ferromagnetism and (anti)ferroelectricity makes multiferroics of interest for applications of integrated logic and data storage devices. Single-phase materials combining multiple of these different "ferroic" properties are called "multiferroics". Usually, magnetism and ferroelectricity are not compatible with each other, and multiferroic materials are very rare in nature. Nonetheless, we now know some systems in which these properties can coexist, including the following examples covered in this review. Undoubtedly, more and more new materials will be discovered in the near future thanks to the upsurge of interest in the past decade. In 2003, the discoveries of two multiferroic materials have triggered an extensive study all over the world on the understanding and application for the next-generation magnetoelectric devices because of their electric/magnetic field control of magnetic/electric properties. The first one was the discovery of large ferroelectric (FE) polarization in epitaxially grown thin films of $BiFeO_3$ which possesses magnetic ordering in the same single-phase material [1]. While the second one was from the magnetic control of FE polarization with a cycloidal spin structure of Mn^{3+} ions in the orthorhombic (*Pbnm*) $TbMnO_3$ [2]. These two ABO_3 perovskites are representatives of type I and type II multiferroics, respectively [3]. On the one hand, $BiFeO_3$ possesses simultaneously high magnetic transition temperature (about 640 K) and high FE Curie temperature T_c (about 1,100 K) [4–6]. The polarization of $TbMnO_3$ $\sim$0.06 μC/cm^2 is much smaller than $BiFeO_3$ $\sim$100 μC/cm^2 by several orders of magnitude. On the other hand, the magnetoelectric coupling in bulk BFO is very weak [7] in comparison with $TbMnO_3$. Coupling between magnetic and FE order is generally strong in these so-called type II materials where the ferroelectricity arises

Published online: 11 October 2014

due to certain type of magnetic spin structures. The readers are referred to a review work on some multiferroic perovskite manganites with ferroelectricity driven by magnetic orders [8].

The discussion of searching multiferroics from rare earth and transition metal perovskite oxides (RMO_3) is the main topic of this review. Over the past decades, RMO_3 materials have been enormously reported. In particular, they show a wide range of electronic, magnetic, optical, and mechanical effects. Such complex oxides containing rare earth and transition metal display an unparalleled richness of physical phenomena arising from the coupling of their charge, spin, and orbital degrees of freedom. Typical flagship materials include yttrium barium copper oxide (YBCO) for cuprate high T_c superconductors and lanthanum manganite ($LaMnO_3$) for colossal magnetoresistive (CMR) materials. RMO_3 are indeed a big class of materials with the simple chemical formula, where R is a rare earth element (from 15 lanthanides La, Ce, Pr, Nd, Pm, Sm, Eu, Gd, Tb, Dy, Ho, Er, Tm, Yb, Lu, and two chemically similar Sc and Y) and M is a transition metal. These materials generally have the perovskite structure shown in Fig. 1a, consisting of MO_6 octahedra which share corners infinitely in all three dimensions. The R cations occupy every hole that is created by eight MO_6 octahedra, giving the R cation a 12-fold oxygen coordination, and the M cation a sixfold oxygen coordination (M is located inside a six-oxygen octahedral cage). There are many ABO_3-type compounds for which the ideal cubic structure is distorted to a lower symmetry (e.g., tetragonal, orthorhombic, rhombohedral, etc.). The combinations by choosing different rare earth R and transition metal M elements make a large amount of materials, hence it is difficult to include all possible such materials in this paper. Our main aim is to give a general overview and to showcase some outstanding candidates to combine magnetism and ferroelectricity, without an attempt to make exhausted survey of this fast developing field. From practical application point of view, we also consider to predict a new class of multiferroics at room temperature consisting of oxide superlattices whose electrical and ferromagnetic (FM) properties can be easily controlled.

In addition to pure RMO_3, another topic of interest to mention is about solid solutions made from the substitution by rare earth R elements in other ABO_3 materials. The resulting material can exhibit a compositionally induced structural phase transition, which is accompanied by enhanced electromechanical response and dielectric constant. This structural transition is attributed to a chemical pressure originating from the ionic radii mismatch between R- and A-site atoms. R can thus be used as substitution doping [10, 11] element for tailoring the multiferroic

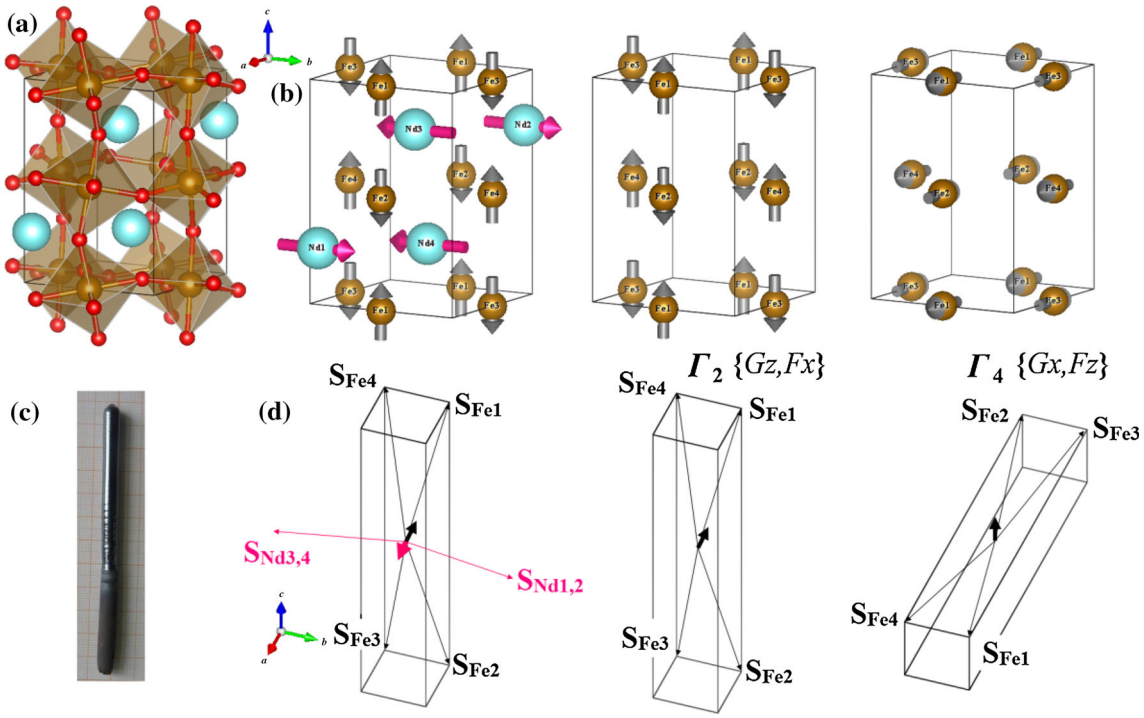

Fig. 1 Crystal structure with orthorhombic *Pbnm* space group symmetry, magnetic configurations of $NdFeO_3$ sample. **a** A unit cell of $NdFeO_3$ crystal structure (Cyan: Nd, Brown: Fe, Red: O), **b** antiferromagnetic (AFM) spin structures for Γ_2 (low temperature) and Γ_4 (high temperature) configurations, **c** $NdFeO_3$ single crystal grown at Shanghai University by optical floating zone method, **d** the arrows are exaggerated for illustrating more clearly the weak ferromagnetisms resulted from the canted AFM orders in **b**. Reprinted with permission from [9]. Copyright 2013 by the American Physical Society

polarization vectors. The rest of the paper is organized as follows. In Section 2, we discuss some recent findings of RMO_3 crystals showing possible multiferroic properties. In Section 3, we briefly discuss the epitaxial strain engineering to trigger some novel FM multiferroics. In Section 4, we present atomistic design and understanding of some exotic perovskite superlattice models. Section 5 is devoted to a conclusion of this review.

2 Rare earth orthoferrites and orthochromites

RMO_3 perovskite oxides are often orthorhombically distorted from the ideal cubic crystal lattice and show temperature-dependent structural and magnetic phase transitions. RMO_3 containing rare earth and transition metal can exhibit interesting magnetic, structural, and transport properties. It is well known that their magnetic properties are sensitive to temperature, magnetic field, and photoinduction. The interaction between the two magnetic subsystems of the R and M sublattices (when R 4f electrons and M 3d electrons are partially filled) and the anisotropic constants can lead to a series of easy axis rotation (spin reorientation) phase transitions upon cooling down below the Neel temperature T_N (usually 620–740 K for M = Fe, 110–280 K for M = Cr). When the subsystem of iron ions orders at T_N, a weak ferromagnetism caused by canting of the spin structures in such essentially AFM structures, points along the c axis (z direction) of the crystal. The magnetocrystalline symmetry thus presents $\Gamma_4(G_x,F_z)$ configuration in rare earth orthoferrites or orthochromites. Remarkably, many $RFeO_3$ crystals exhibit characteristic spin reorientation transitions upon cooling, mostly $\Gamma_4(G_x,F_z) \rightarrow \Gamma_{24}(G_{x,z},F_{x,z}) \rightarrow \Gamma_2(G_z,F_x)$ occurring in the temperature interval $[T_2,T_1]$ with $T_2 < T_1 < T_N$ [9, 12–14] as shown in Fig. 1.

Except when R = La, Lu, Y with fully unoccupied or fully occupied f electrons, the net moment of the R spins is polarized parallel or antiparallel to the net M moment by the R–M magnetic interactions. Thus a magnetic compensation (zero magnetization) and magnetic reversal with decreasing temperature can be attributed to the antiparallel coupling between R and M moments. We take single-crystal $NdFeO_3$ as an example here, which features two nonequivalent magnetic sublattices, namely Fe and Nd magnetic moments that are coupled in an antiparallel fashion. There exists an interaction between 3d and 4f electrons of these two sublattices along with a spin–lattice coupling which is strongly sensitive to the history and orientation of applied weak magnetic field. More details of intriguing spin switching phenomena can be found in Ref. [9]. So far, almost all rare earth orthoferrite $RFeO_3$ single crystals have been successfully grown at Shanghai University, from a four-mirror optical floating zone furnace ion using four 1.5 kW halogen lamps as the infrared radiation source with flowing air. The temperature of the molten zone was precisely controlled by adjusting the power of the lamps. During the growth process, the molten zone moved upwards, with the seed rod (lower shaft) and the feed rod (upper shaft) counter rotating in a gas flow. The compositional homogeneity and crystal morphology analyzed by X-ray diffraction (XRD) and scanning electron microscopy (SEM) with energy-dispersive X-ray spectroscopy (EDX) have been used to confirm the high quality of the single crystals [15–17].

First-principles calculations based on the density functional theory (DFT) have become an indispensable tool to predict and explain many physical properties. We have studied the evolution of the structural parameters and physical properties of RMO_3 (M = Fe, Cr) perovskites, for a systematic understanding on these systems. Taken the rare earth ionic radius as a variable, the dependence of structural and magnetic properties of rare earth orthoferrites (of *Pbnm* ground state) is comprehensively investigated from first principles [14]. We have reproduced such "chemical pressure"-induced (i.e., rare earth ionic radius) changes on the lattice constants, Fe–O bond lengths, Fe–O–Fe bond angles, and Fe–O bond length splittings by DFT calculations. Our simulations have also offered novel predictions on tiltings of FeO_6 octahedra, cation antipolar displacements, and weak magnetization that can be checked experimentally. Particularly, a linear relationship between the weak FM moment of $RFeO_3$ and the rare earth ionic radius was found. Figure 2 shows the quantities of magnetic moment and FeO_6 tilting versus rare earth radius [14]. Further, we also theoretically applied hydrostatic pressure to look at structural and magnetic behavior of $SmFeO_3$ as well. Unlike previously assumed, hydrostatic pressure generates changes of physical properties that are quantitatively and even qualitatively different from those associated with the chemical pressure. We have also reported a systematic investigation of orthorhombic perovskite $RCrO_3$ by first principles calculations for different rare earth R^{3+} cations [18]. The calculations are carried out to investigate structural and magnetic behaviors of rare earth orthochromates as a function of "chemical" pressure, epitaxial misfit strain, and hydrostatic pressure. Briefly, we found that the "chemical" pressure significantly changes antipolar displacements, Cr–O–Cr bond angles and the resulting oxygen octahedral tiltings, while the hydrostatic pressure mostly modifies Cr–O bond lengths, and the misfit strain affects all these quantities. The correlations between magnetic properties (T_N and weak FM) and unit cell volume are similar when varying the misfit strain or hydrostatic pressure, but differ from that associated with the "chemical" pressure. One can see that for the orthorhombic perovskites in general, hybridization between the M cation

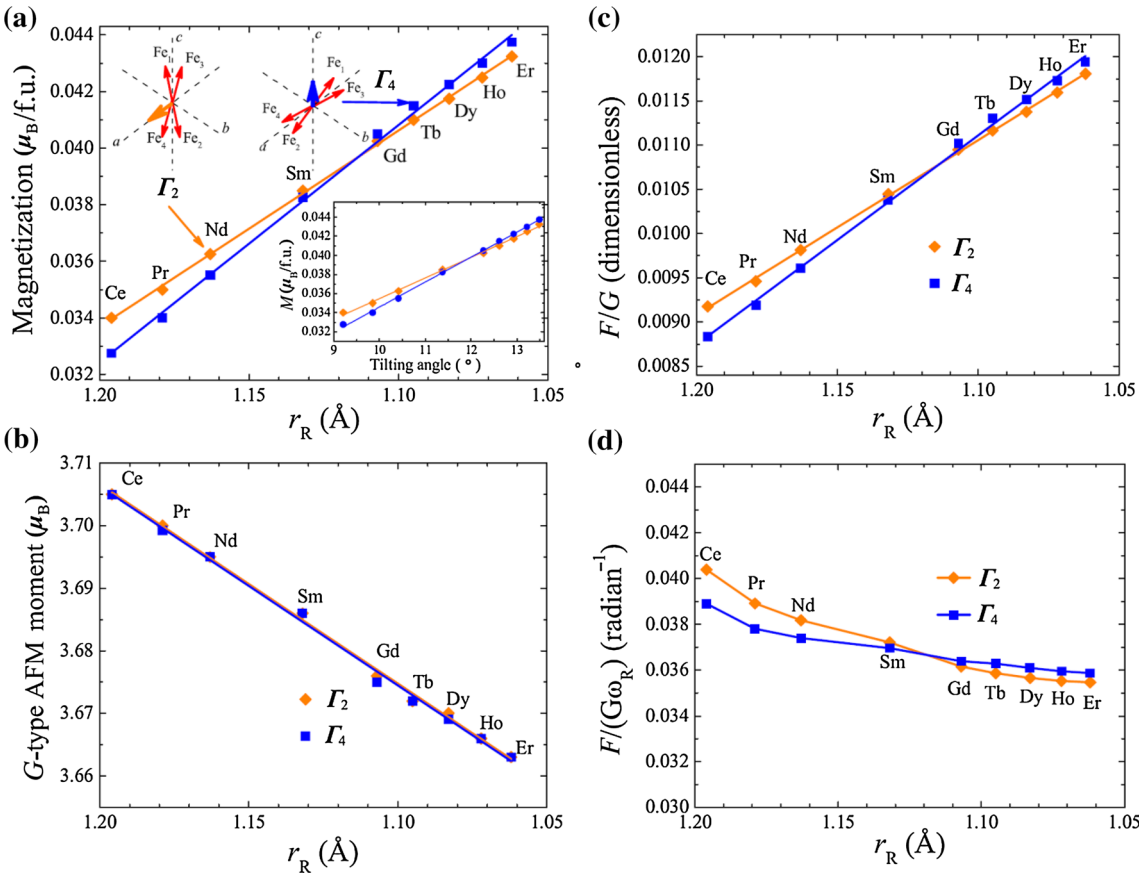

Fig. 2 (Color online) The Γ_2- and Γ_4-magnetic configurations of $RFeO_3$ versus the rare earth ionic radius. **a** and **b** show the magnitudes of weak magnetization and *G*-type AFM vectors of Fe, respectively, **c** shows the ratio between FM and AFM moments, and **d** represents the division of this ratio by the magnitude of the anti-phase tilting angle (in radian). The insets of **a** show the Γ_2- and Γ_4-magnetic configurations and their magnetizations as a function of the anti-phase tilting angle (about the pseudocubic [100] or [010] direction) of the FeO_6 octahedron. Reprinted with permission from [14]. Copyright 2013 by IOP Publishing Ltd

and O is essential to weaken the short-range repulsion and allow the distortion. In addition, the R cation can modify the ground state and nature of the transition by hybridizing with the valence state, leading indirectly to changes in the M–O interactions. Furthermore, if the size of the R ions becomes smaller, the crystal structure is more distorted that will change the spin-exchange energies and modify the magnetic properties accordingly [19].

$GdFeO_3$, as an orthodox perovskite oxide, possesses a not only weak FM but also FE ground state, in which the FE polarization is generated by the striction through the exchange interaction between the Gd and Fe spins [20]. It is remarkable that FE polarization and magnetization are successfully controlled by magnetic and electric fields, respectively. Such unprecedented mutual controllability of electricity and magnetism is attributed to the unique feature of composite (electric and magnetic) domain walls clamping. Magnetoelectric phenomena have also been found in a single crystal of $DyFeO_3$. Below the AFM ordering temperature of Dy moments, a large linear-ME tensor component is observed. Further, a magnetic field along the *c* axis induces a multiferroic phase (weakly FM and FE) both along the *c* axis [21]. By performing accurate ab initio calculations, the role of 4f electrons in stabilizing the magnetic-field-induced FE state of $DyFeO_3$ was studied and cross-checked with the DFT+U, the Heyd–Scuseria–Ernzerhof (HSE) hybrid functional and the so-called GW approaches [22]. The FE polarization is confirmed to be driven by an exchange-strictive mechanism, between adjacent spin-polarized Fe and Dy layers with the respective layered AFM components. A careful electronic structure analysis suggests that coupling between Dy and Fe spin sublattices is mediated by Dy–d and O–2p hybridization. These findings indicate that the interaction between the f and d sublattices might be used to tailor the FE and magnetic properties of multiferroic compounds [22]. A more recent study on $DyFeO_3$ revealed that ferroelectricity exists in the weak FM state and disappears below the spin reorientation transition without applying a magnetic field, thus suggesting the crucial role of weak ferromagnetism in inducing ferroelectricity [23].

$SmFeO_3$, a rare earth orthoferrite having the highest spin reorientation (from *c*-axis to *a*-axis) temperature at

$T_{SR} = 480$ K, was reported to exhibit ferroelectricity below T_N^{Fe} (670 K) of iron [24, 25]. This is surprising since rare earth moments order at low temperatures (<10 K), and the mechanism discussed above may not directly account for the origin of ferroelectricity at such high temperature. And if we employ the $S_i \times S_j$-type spin-current or the inverse Dzyaloshinskii–Moriya (DM) interaction model for such a canted AFM system, it leads to non-FE state because local polarization cancels out by the alternate arrangement of pairs of canted spins. Instead, $S_i \times S_j$-type exchange striction mechanism is primarily responsible for the observed improper FE polarization of $SmFeO_3$ [26, 27]. Very recently, epitaxial growth of thin-film $SmFeO_3/SrRuO_3$ was achieved on $SrTiO_3$ substrates by the pulsed laser deposition (PLD) method on a single-crystal $SrTiO_3$ substrate. The polarization–electric field (*P*–*E*) loop was measured and claimed to outperform the bulk sample [28]. However, we must emphasize that further investigations are very necessary for better understanding these results, and the determining roles of rare earth and transition metal ions involved as well.

When the size of the R ions becomes smaller, the crystal structure is more distorted which will change the spin-exchange energies and modify the magnetic properties accordingly. $YbFeO_3$ thin-film heterostructure fabricated by adopting a hexagonal template also surprisingly exhibits nonferroelastic ferroelectricity with T_c of 470 K [29]. The observed ferroelectricity has been further characterized by an extraordinary two-step polarization decay, accompanied by a pronounced magnetocapacitance effect near the lower decay temperature, ~225 K. According to first-principles calculations, the hexagonal $P6_3/mmc$–$P6_3mc$–$P6_3cm$ consecutive transitions are primarily responsible for the observation, and the ferroelectricity originates from the *c*-axis-oriented asymmetric Yb $5d_z^2$–O $2p_z$ orbital hybridization. Similarly, single-crystalline hexagonal $LuFeO_3$ films are found to be polar and switchable at room temperature [30]. The AFM order is shown to occur below 440 K, followed by a spin reorientation resulting in a weak FM order below 130 K. The finding of such coexisting multiple ferroic orders demonstrates that hexagonal $LuFeO_3$ films are also room-temperature multiferroics.

3 Rare earth titanate under epitaxial strains

As mentioned above, epitaxial strain has been successful as a route to obtain novel ferroelectrics in thin films, where lattice mismatch between the substrate and overlayer is used to modify properties that are very different from the bulk. For instance, the substrate strain could be used to generate a FE ground state in the nonmagnetic paraelectric $SrTiO_3$ [31]. Same schemes also work for multiferroics, for instance, epitaxial strain may transform simple rocksalt binary oxides such as EuO [32], as well as $SrMnO_3$ [33] and $EuTiO_3$ [34, 35], to FE materials. First-principles calculations [36] even predict that by simply depositing the room-temperature FM double perovskites Bi_2NiReO_6 and Bi_2MnReO_6 on a substrate strain should turn their antipolar bulk ground state into a FE one. For the materials already showing bulk FE, strain engineering has also been shown to be a powerful and flexible means of tailoring the properties of ABO_3 thin films [37, 38] or superlattices [39]. The effect of epitaxial strain on the structure of the perovskite unit cell can induce a host of interesting effects, arising from either polar cation shifts or rotation of the oxygen octahedra, or both. In the multiferroic perovskite bismuth ferrite $BiFeO_3$, both degrees of freedom exist, and thus desirable effects may be expected as one plays with epitaxial strain [40]. For instance, a compressive strain can induce a polarization rotation from [111] toward [001] direction, accompanied by a huge *c*/*a* tetragonal ratio of about 1.3 and five-fold coordinated Fe atoms [40–42]. A tensile strain can introduce a new state of orthorhombic $Pmc2_1$ symmetry that is characterized by a large in-plane polarization coexisting with oxygen octahedra tilting in-phase about the *z* direction [43].

Due to their magnetoelectric properties, perovskite oxides with divalent europium (Eu^{2+}) have been brought to attention in the past decades. Though bulk $EuTiO_3$ is not multiferroic by exhibiting a *G*-type AFM ordering below 5.3 K and paraelectric down to 0 K, epitaxial (001) $EuTiO_3$ films can become both FE and FM under large enough misfit strain [34, 35]. We have performed more accurate ab initio computations to investigate the properties of bulk material and epitaxial films and found a rich phase diagram of $EuTiO_3$ films [43]. Consistent with a recent experiment [44] and in contrast to what was previously believed, the bulk $EuTiO_3$ ground state is not cubic *Pm*-3*m* but is tetragonal *I*4/*mcm* instead by displaying oxygen octahedra tiltings. Furthermore, anomalous AFE patterns were found to coexist with the modulated tilting [45]. Figure 3a shows the calculated total energy of several states as a function of misfit strain. The energy difference between FM and AFM of these crystallographic states is shown in Fig. 3b, in which negative values indicate a more preferable FM state over AFM state. Figure 3c, d shows Cartesian components of the FE polarization calculated from the modern theory of polarization [46], and of the oxygen octahedral anti-phase antiferrodistortive (AAFD) vector, respectively. The inset of Fig. 3d displays Cartesian components of the in-phase antiferrodistortive (IAFD) vector. Here, the AAFD and IAFD vectors are defined such that their axes provide the direction about which oxygen octahedral tilt anti-phase and in-phase, respectively, while their magnitudes provide the angle of such tilting. The *x*, *y*, and *z* axis are along the pseudocubic [100], [010], and [001] directions, respectively.

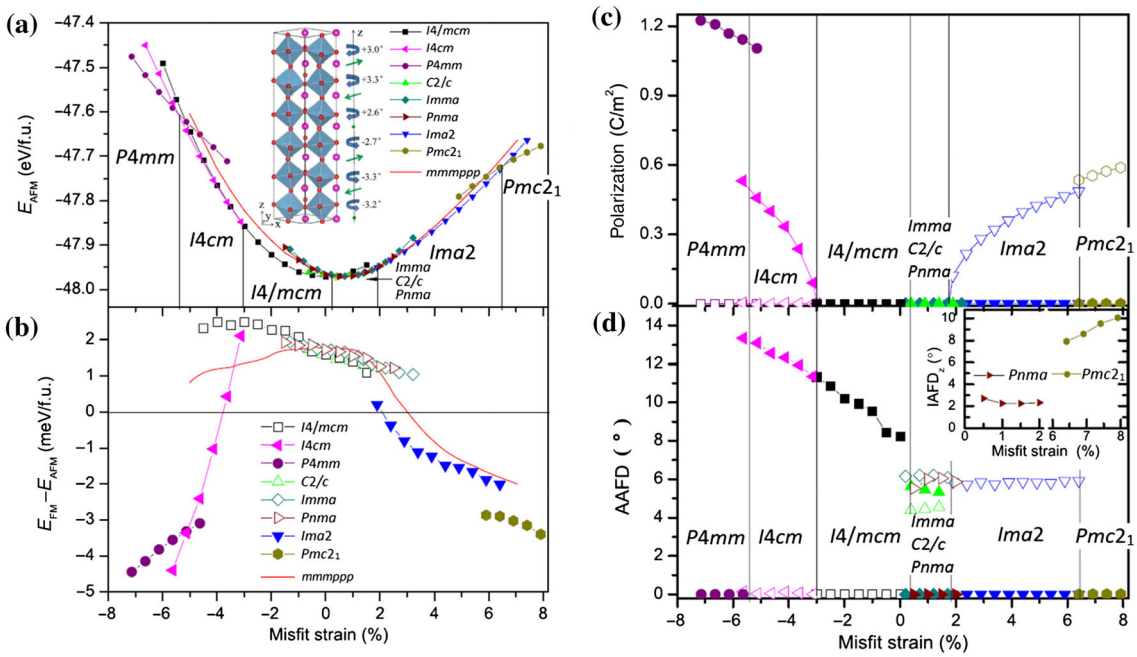

Fig. 3 (Color online) Calculated energies of the *G*-type AFM state (**a**) and energy difference between the *G*-type AFM and FM states (**b**) as function of the biaxial strain for different phases in epitaxial (001) $EuTiO_3$ films. The inset of (**a**) displays schematically nanoscale twinned phases of the complex tilting pattern, and the curled and straight arrows representing oxygen octahedra tilting and antipolar Eu displacements, respectively. Evolution of the polarization (**c**) and anti-phase AAFD vector (**d**) with strain for equilibrium phases. The inset of (**d**) shows the IAFD vector of the *Pnma* and *Pmc*2_1 state. Open symbols display the *x* or *y* component, solid symbols show the *z* component. Reprinted with permission from [43]. Copyright 2012 by the American Physical Society

We can see that for compressive strain between 0 % and −3 %, $EuTiO_3$ films adopt a tetragonal *I*4/*mcm* state, with a *G*-type AFM ordering of Eu atoms, as the paraelectric ground state. At the same time, the *I*4/*mcm* phase has a non-vanishing *z* component of AAFD vector which increases from ∼8° to ∼11° as shown in Fig. 3d. Upon further compressive strain from −3 %, $EuTiO_3$ film undergoes a second-order phase transition from *I*4/*mcm* phase to *I*4*cm* state, which is characterized by the appearance of an out-of-plane component of polarization (Fig. 3c) in addition to the preexisting out-of-plane AAFD vector. Both of these out-of-plane components increase as the compressive strain changes from −3 % to −5.4 %. Strikingly, the *I*4*cm* state adopts an AFM ordering for strain between −3 % and −3.8 %, while becomes FM for compressive strain beyond this magnitude. The magnetic transition therefore occurs at about −3.8 % within the same structural phase (namely, *I*4*cm*). Moreover, at −5.4 %, a first-order strain-driven phase transition from this tetragonal *I*4*cm* phase to a tetragonal *P*4*mm* phase occurs (both showing FM order). Finally, in this *P*4*mm* state (similar as $PbTiO_3$), the AAFD vector is annihilated and the polarization along *z* direction is increasing for compressive strain from −5.4 % to −7 %.

On the tensile strain side, Fig. 3a, b reveal three *G*-AFM phases that are almost degenerate in energy and lower than *I*4/*mcm*, namely the orthorhombic *Imma*, *Pnma*, and monoclinic *C*2/*c*, for strain ranging between 0.25 % and 1.9 %. Specifically, the *Imma* state has a significant in-plane AAFD vector with equal *x* and *y* components of 6.2°. The *C*2/*c* state has both in-plane (4.5° for both *x* and *y* directions) and out-of-plane (5.5°) components of the AAFD vector. Moreover, the *Pnma* state has in-plane AAFD of 6° and out-of-plane IAFD of 2.5° in this strain range. For larger strain between 1.9 % and 6.5 %, the ground state of epitaxial $EuTiO_3$ films transforms from AFM to FM and becomes orthorhombic *Ima*2. Interestingly, it also presents a FE polarization along the in-plane [110] direction that increases with strain strength. These DFT results therefore reproduce previous experimental results [34] that a tensile strain can introduce coexistence of both FE and FM. At even larger tensile strain of 6.5 %, there appears a first-order phase transition from *Ima*2 to a state of *Pmc*2_1. Such a common state has also been found in tensile-strained $BiFeO_3$ and $PbTiO_3$ films [43]. As in *Ima*2, it is FE in-plane along [110] direction and is also FM. Different from *Ima*2, the *Pmc*2_1 state possesses a vanishing AAFD vector but exhibiting in-phase rotation about the *z* axis. The resulting rotation angle has a magnitude of ∼8° near the transition and further increases with the tensile strain. Some recent results in Ref. [47] are in agreement with our findings [43].

4 Hybrid improper multiferroics from superlattice

In 2008, a FE/paraelectric $PbTiO_3/SrTiO_3$ superlattice with very short periods was found to possess a new form of interface coupling from oxygen rotational distortions, which gives rise to "improper" ferroelectricity [48]. Since then such an approach based on the interface engineering has generated increasing interest to produce artificial multilayered materials with unique properties. Very recently, the discovery of a new form of ferroelectricity in some $A'BO_3/A''BO_3$ perovskite oxide artificial superlattices, now termed hybrid improper ferroelectricy (HIF) [49], has been attracting a lot of attention. The fact that HIF can also be used to electrically control magnetism in some of these superlattices further emphasizes its fundamental and technological importance especially for multiferroics [50]. From a phenomenological perspective, the appearance of HIF was found to rely on a trilinear coupling term of the form PQ_1Q_2, where P is the electric polarization (zone-center mode) while Q_1 and Q_2 are two non-polar (zone-boundary) modes. Examples of the latter are the oxygen octahedral rotations that are ubiquitous in perovskite oxides, as seen in $RFeO_3$ and $EuTiO_3$ above. The simultaneous occurrence of such rotations in-phase (Q_1) and in anti-phase (Q_2) is what gives rise to an electric polarization, via the PQ_1Q_2 coupling, in the "classic" HIF materials. The pioneering works on HIF derived this trilinear energy from symmetry arguments involving macroscopic order parameters, following the usual Landau theory approach. The same kind of methodology has been recently used to discuss how HIF results from the disruption caused by the chemical order inherent to the superlattices of an anti-ferroelectric pattern.

Our latest results provide an alternative viewpoint to the previously published Laudau theory-based works [51]. We now discuss the so-called hybrid improper ferroelectricity appearing in $A'BO_3/A''BO_3$ perovskite superlattices. By means of straightforward analytical derivations and associated graphical analysis, we demonstrate that two previously proposed elemental interatomic couplings between the O_6 octahedral rotations and the displacements of the A-site cations [52] naturally reproduce and explain HIF in $(A'BO_3)_1/(A''BO_3)_1$ superlattices composed of layers that are only one unit cell thick. From this atomistic coupling energy, we can deduce the forces acting on the atoms and thus the proportional distortion (and polarization) of the structure. Further, we show that our approach permits an easy treatment of superlattices of arbitrary stacking direction and layer thickness. In particular, this allows us to predict other previously overlooked types of HIF in $(A'BO_3)_1/(A''BO_3)_1$ superlattices. By discretizing the magnitude of the spontaneous polarization in $(A'BO_3)_m/(A''BO_3)_n$ systems when varying the m and n layer thicknesses, we found a rule for emergence of HIF where m/n must take odd/odd integer numbers (the corresponding polar space group being $Pmc2_1$). In other words, the polarization is zero when both m and n are even (the resulting paraelectric phase has $P2_1/c$ symmetry) and when m and n have different parity (the resulting state presents the $Pbnm$ space group). We show from first-principles polarization results confirming all these interesting predictions quantitatively [51] (Fig. 4).

It is particularly important to discover materials that possess electrical polarization and are FM at high or even room temperature. From DFT, the properties of as-yet-unsynthesized 3d–5d ordered double perovskites ($A_2BB'O_6$) have been explored with highly polarizable Bi^{3+} ions on the A site [36]. It was found that the insulating Bi_2NiReO_6 and Bi_2MnReO_6 compounds exhibit a robust net magnetization that persists above room temperature. When the pseudocubic in-plane lattice vectors are constrained to be orthogonal by coherent epitaxy, the ground states are strongly FE.

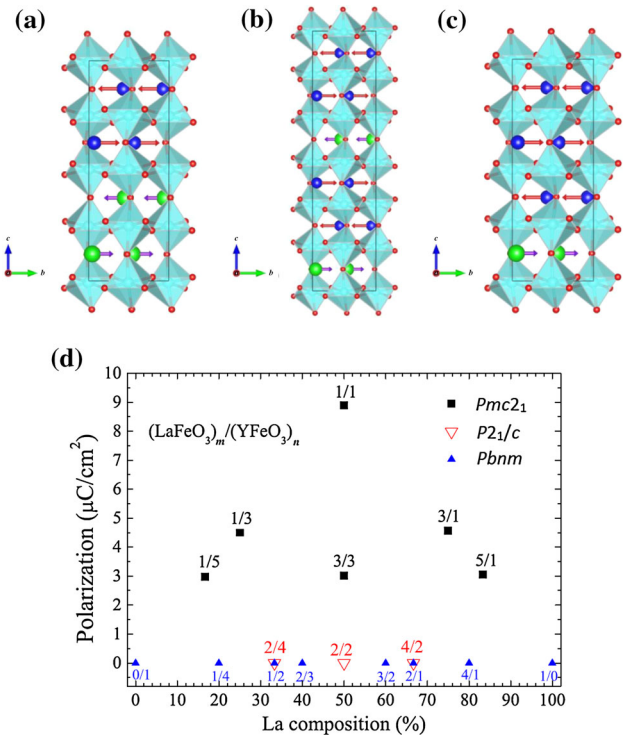

Fig. 4 (Color online) **a–c** sketch of the antipolar displacements associated with the HIF energy in (001) $(A'BO_3)_m/(A''BO_3)_n$ superlattices, for which both $A'BO_3$ and $A''BO_3$ materials have $a^-a^-c^+$ tilting pattern. **a** Corresponds to the case when both n and m are even, and shows that no polarization can exist since antipolar motions precisely cancel each other in the A′O and A″O layers (2/2); **b** represents the case when n and m are of different parity, which also results in a vanishing polarization (1/2); **c** shows the unique case in which HIF can occur, that is when n and m are both odd (1/3). **d** Magnitude of the polarization of (001) $(LaFeO_3)_n/(YFeO_3)_m$ superlattice as a function of La composition, for different combinations of n and m. Reprinted with permission from [51]. Copyright 2014 by the American Physical Society

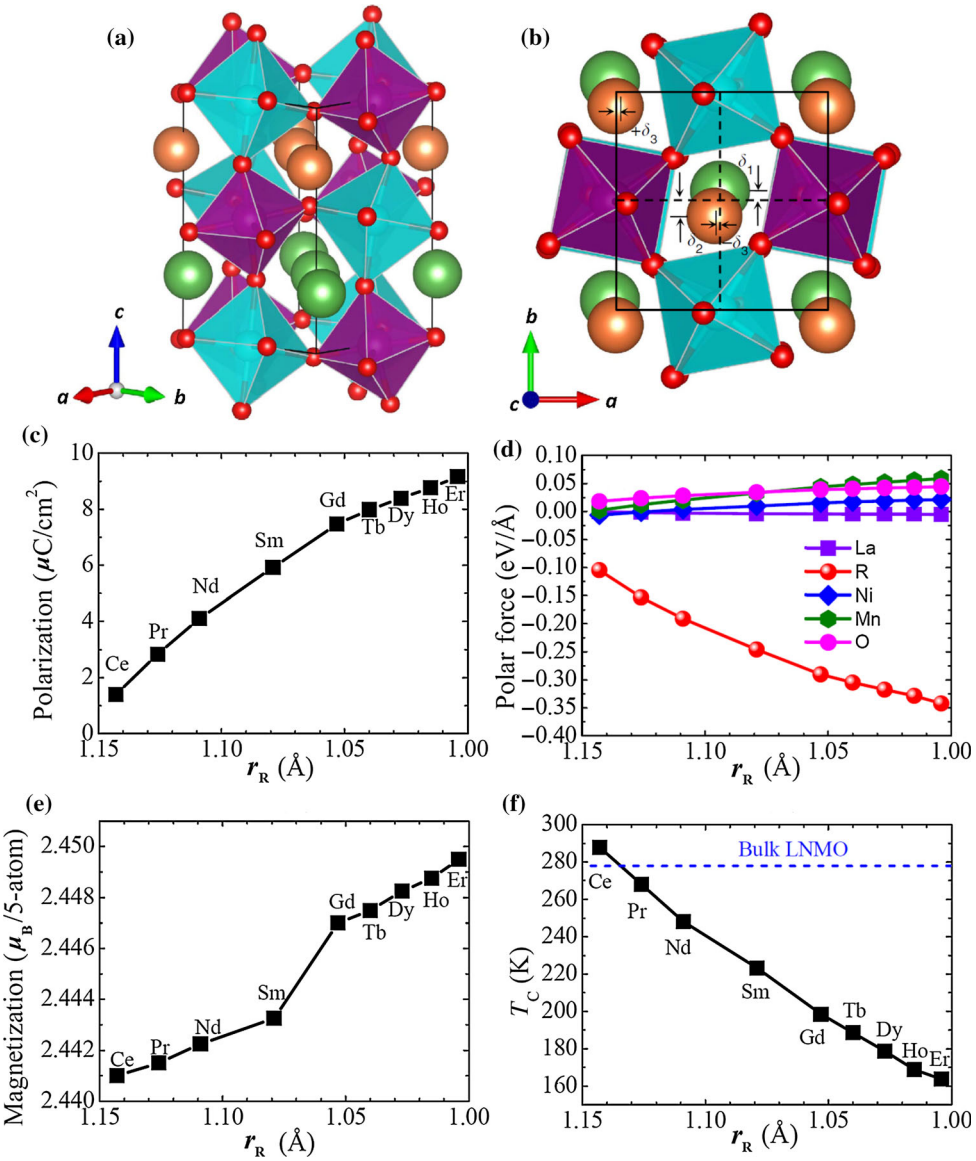

Fig. 5 $P2_1$ ground state of the studied R_2NiMnO_6/La_2NiMnO_6 superlattices in three dimensions (**a**) and in the (*a*, *b*) plane (**b**). The La^{3+}, R^{3+}, Ni^{2+}, Mn^{4+}, and O^{2-} ions are displayed as green, orange, cyan, purple, and red spheres, respectively. The NiO_6 and MnO_6 octahedra are displayed using cyan and purple octahedra, respectively. The largest magnitude of the antipolar displacement δ_2 of the R^{3+} ions with respect to those δ_1 of the La^{3+} ions along the *b*-axis is schematized here, in order to emphasize that this inhomogeneity is the microscopic reason for the creation of the electrical polarization. The antipolar displacements along the *a*-axis of the R ions within the RO plane (denoted as $+\delta_3$ and $-\delta_3$) are also shown [56]

There is also a large uniaxial magnetocrystalline anisotropy with easy axis along the FE polarization direction. However, both the Re and Ni/Mn sublattices adopt an AFM order, therefore yielding a FM rather than FM overall ordering near 300 K. Similarly, ferrimagnetism (or weak magnetization) instead of ferromagnetism occurs in other compounds possessing a room-temperature electrical polarization; that is the case of $GaFeO_3$ [53], hexagonal $LuFeO_3$ epitaxial thin films [30], and the solid solutions formed by mixing lead zirconium titanate and lead iron tantalite (PZTFT) perovskites [54]. Therefore, systems exhibiting both a significant electrical polarization and a strong magnetization near room temperature are very scarce and desirable [55, 56].

On the other hand, double perovskite Bi_2NiMnO_6 has been recently synthesized and found to be FE below 485 K and FM below 140 K [57]. The next step will naturally be realizing the possibility of ferromagnets having a polarization near 300 K. Double perovskite oxides R_2NiMnO_6 are good candidates, especially because La_2NiMnO_6 has a FM Curie temperature $T_{cm} \sim 287$ K and T_{cm} is nearly linearly dependent on the radius of the rare earth ion in R_2NiMnO_6 [58]. Unfortunately, R_2NiMnO_6 systems are not FE but rather possess antipolar displacements resulting

from their oxygen octahedral tilting pattern ($a^-a^-c^+$ in Glazer's notation). Nevertheless, by mixing them with La_2NiMnO_6 compounds to form short-period (001)-oriented R_2NiMnO_6/La_2NiMnO_6, superlattices are capable of inducing a spontaneous electrical polarization at room temperature. Again, we resort to HIF methodology to make (001)-oriented $(ABO_3)_1/(A'BO_3)_1$ superlattices exhibit an electrical polarization if both ABO_3 and $A'BO_3$ materials adopt $a^-a^-c^+$ tilting pattern. As shown in Fig. 5, (001) R_2NiMnO_6/La_2NiMnO_6 superlattices can indeed be both FM and FE near room temperature. Figure 5a shows the predicted electric polarization (as computed from Berry phase), which can be understood by looking at the average forces (along the *b* direction) on each atom in the unrelaxed state of the superlattice, for which the lattice parameters and atomic coordinates are those of the paraelectric $P2_1/n$ state of La_2NiMnO_6. Figure 5c, d shows the magnetization (at $T = 0$ K) and paramagnetic-to-FM transition temperature (as calculated by Monte Carlo simulation) in the relaxed $P2_1$ ground state of the superlattices, respectively. Moreover, we have showed that their electrical polarization and magnetic T_c can be tuned by varying the chemical pressure (i.e., the size of the rare earth ion) and/or the epitaxial strain imposed by the substrates on which the superlattice films are grown [56]. Importantly, in view of the high critical temperatures associated with the structural and magnetic phase transitions in the parent compounds, we expect that such systems are promising candidate to achieve electric switching of the magnetization at the room temperature. The magnetization will follow if the polarization is switchable, and generally other superlattices possessing the same kind of trilinear coupling energy as here can have their polarization switchable too. Future works devoted to homogenous and inhomogenous switching in our novel systems may constitute an interesting avenue to pursue. The identification of such a candidate room-temperature multiferroics is certainly interesting for many experimentalists, theorists, computational scientists, and engineers because of this discovery of a new class of materials that are multiferroics at room temperature.

5 Conclusions

To conclude, in this review, we discussed novel routes to multiferroics, giving specific examples of rare earth and transition metal perovskite oxide materials. Single-phase magnetoelectric materials are promising candidates for operation by combining charge and spin degrees of freedom and fully exploiting the cross-control of magnetism and polarization without necessity of current flow accompanying energy dissipation. Interplay of long-range magnetic order with polarity in the same structure is a prerequisite for the design of (magnetoelectric) multiferroic materials. There are now several demonstrated strategies to achieve this goal, but retaining FM multiferroic order above room temperature remains a difficult target in experiment. To attain applicable magnetoelectric coupling in such materials, the electric polarization would be preferably induced by magnetic order. Along this line, type II multiferroics, in which polarization is caused by a particular type of magnetic structure, satisfy the requirement well. The structural, electric, and magnetic properties of materials in this review have been widely researched in recent years; meanwhile, the pursuit toward room-temperature multiferroics is still facing many challenges. We hope this overview will stimulate more efforts from experimentalists and theorists to work together for the future developments in fundamental science and device applications. These experimental and theoretical approaches will open up new possibilities for exploring, modeling, and exploiting novel electromagnetism and multiferroic materials [59, 60].

Acknowledgements This work was supported by the National Basic Research Program of China (2015CB921600), the National Natural Science Foundation of China (51372149, 50932003, 11274221, 11274222), Qi Ming Xing Project from Shanghai Municipal Science and Technology Commission (14QA1402000), Eastern Scholar Program and Shu Guang Program (12SG34) from Shanghai Municipal Education Commission. We also acknowledge High Performance Computing Platform of Shanghai University and Shanghai Supercomputer Center.

References

1. Wang J, Neaton JB, Zheng H et al (2003) Epitaxial $BiFeO_3$ multiferroic thin film heterostructures. Science 299:1719–1722
2. Kimura T, Goto T, Shintani H et al (2003) Magnetic control of ferroelectric polarization. Nature 426:55–58
3. Khomskii DI (2006) Multiferroics: different ways to combine magnetism and ferroelectricity. J Magn Magn Mater 306:1–8
4. Albrecht D, Lisenkov S, Ren W et al (2010) Ferromagnetism in multiferroic $BiFeO_3$ films: a first-principles-based study. Phys Rev B 81:140401
5. Ren W (2013) Nanodots of multiferroic oxide material $BiFeO_3$ from the first principles. Adv Manuf 1:166–175
6. Ren W, Bellaiche L (2010) Size effects in multiferroic $BiFeO_3$ nanodots: a first-principles-based study. Phys Rev B 82:113403
7. Ren W, Bellaiche L (2011) Prediction of the magnetotoroidic effect from atomistic simulations. Phys Rev Lett 107:127202
8. Dong S, Liu JM (2012) Recent progress of multiferroic perovskite manganites. Mod Phys Lett B 26:1230004
9. Yuan SJ, Ren W, Hong F et al (2013) Spin switching and magnetization reversal in single-crystal $NdFeO_3$. Phys Rev 87:184405
10. Kiat JM, Bogicevic C, Karolak F et al (2010) Low-symmetry phases and loss of relaxation in nanosized lead scandium niobate. Phys Rev B 81:144122
11. Chen W, Ren W, You L et al (2011) Domain structure and in-plane switching in a highly strained $Bi_{0.9}Sm_{0.1}FeO_3$ film. Appl-Phys Lett 99:222904
12. Huang R, Cao S, Ren W et al (2013) Large rotating field entropy change in $ErFeO_3$ single crystal with angular distribution contribution. Appl Phys Lett 103:162412

13. White RL (1969) Review of recent work on the magnetic and spectroscopic properties of the rare-earth orthoferrites. J Appl Phys 40:1061–1069
14. Zhao HJ, Ren W, Yang YR et al (2013) Effect of chemical and hydrostatic pressures on structural and magnetic properties of rare-earth orthoferrites: a first-principles study. J Phys Condens Matter 25:466002
15. Wang X, Cao S, Wang Y et al (2013) Crystal growth and characterization of the rare earth orthoferrite $PrFeO_3$. J Cryst Growth 362:216–219
16. Wang Y, Cao S, Shao M et al (2011) Growth rate dependence of the $NdFeO_3$ single crystal grown by float-zone technique. J Cryst Growth 318:927–931
17. Shao M, Cao S, Wang Y et al (2011) Single crystal growth, magnetic properties and Schottky anomaly of $HoFeO_3$ orthoferrite. J Cryst Growth 318:947–950
18. Zhao HJ, Ren W, Chen XM et al (2013) Effect of chemical pressure, misfit strain and hydrostatic pressure on structural and magnetic behaviors of rare-earth orthochromates. J Phys Condes Matter 25:385604
19. Mekam D, Kacimi S, Djermouni M et al (2012) Ab initio calculations on RE–TM–O_3 perovskites: a comparative study of cation effect. Results Phys 2:156–163
20. Tokunaga Y, Furukawa N, Sakai H et al (2009) Composite domain walls in a multiferroic perovskite ferrite. Nat Mater 8:558–562
21. Tokunaga Y, Iguchi S, Arima T et al (2008) Magnetic-field-induced ferroelectric state in $DyFeO_3$. Phys Rev Lett 101:097205
22. Alessandro S, Martijn M, Georg K et al (2010) The multiferroic phase of $DyFeO_3$: an ab initio study. New J Phys 12:093026
23. Rajeswaran B, Sanyal D, Mahuya C et al (2013) Interplay of 4f–3d magnetism and ferroelectricity in $DyFeO_3$. Europhys Lett 101:17001
24. Zhao H, Cao S, Huang R et al (2013) Enhanced 4f–3d interaction by Ti-doping on the magnetic properties of perovskite $SmFe_{1-x}Ti_xO_3$. J Appl Phys 114:113907
25. Lee JH, Jeong YK, Park JH et al (2011) Spin-canting-induced improper ferroelectricity and spontaneous magnetization reversal in $SmFeO_3$. Phys Rev Lett 107:117201
26. Johnson RD, Terada N, Radaelli PG (2012) Comment on "spin-canting-induced improper ferroelectricity and spontaneous magnetization reversal in $SmFeO_3$. Phys Rev Lett 108:219701
27. Lee JH, Jeong YK, Park JH et al (2012) Lee et al reply. Phys Rev Lett 108:219702
28. Si W, Huang K, Wu X et al (2014) Epitaxial thin film of $SmFeO_3$ ferroelectric heterostructures. Sci China Chem 57:803–806
29. Jeong YK, Lee JH, Ahn SJ et al (2012) Structurally tailored hexagonal ferroelectricity and multiferroism in epitaxial $YbFeO_3$ thin-film heterostructures. J Am Chem Soc 134:1450–1453
30. Wang W, Zhao J, Wang W et al (2013) Room-temperature multiferroic hexagonal $LuFeO_3$ films. Phys Rev Lett 110:237601
31. Haeni JH, Irvin P, Chang W et al (2004) Room-temperature ferroelectricity in strained $SrTiO_3$. Nature 430:758–761
32. Bousquet E, Spaldin NA, Ghosez P (2010) Strain-induced ferroelectricity in simple rocksalt binary oxides. Phys Rev Lett 104:037601
33. Lee JH, Rabe KM (2010) Epitaxial-strain-induced multiferroicity in $SrMnO_3$ from first principles. Phys Rev Lett 104:207204
34. Lee JH, Fang L, Vlahos E et al (2010) A strong ferroelectric ferromagnet created by means of spin–lattice coupling. Nature 466:954–958
35. Fennie CJ, Rabe KM (2006) Magnetic and electric phase control in epitaxial $EuTiO_3$ from First principles. Phys Rev Lett 97:267602
36. Ležaić M, Spaldin NA (2011) High-temperature multiferroicity and strong magnetocrystalline anisotropy in 3d–5d double perovskites. Phys Rev B 83:024410
37. Sando D, Agbelele A, Daumont C et al (2014) Control of ferroelectricity and magnetism in multi-ferroic $BiFeO_3$ by epitaxial strain. Philos Trans R Soc A Math Phys Eng Sci 372:20120438
38. Daumont C, Ren W, Infante IC et al (2012) Strain dependence of polarization and piezoelectric response in epitaxial $BiFeO_3$ thin films. J Phys Condens Matter 24:162202
39. Yang Y, Ren W, Stengel M et al (2012) Revisiting properties of ferroelectric and multiferroic thin films under tensile strain from first principles. Phys Rev Lett 109:057602
40. Ren W, Yang Y, Diéguez O et al (2013) Ferroelectric domains in multiferroic $BiFeO_3$ films under epitaxial strains. Phys Rev Lett 110:187601
41. Chen Z, Zou X, Ren W et al (2012) Study of strain effect on in-plane polarization in epitaxial $BiFeO_3$ thin films using planar electrodes. Phys RevB 86:235125
42. Chen Z, Prosandeev S, Luo ZL et al (2011) Coexistence of ferroelectric triclinic phases in highly strained $BiFeO_3$ films. Phys Rev B 84:094116
43. Yang Y, Ren W, Wang D et al (2012) Understanding and revisiting properties of $EuTiO_3$ bulk material and films from first principles. Phys Rev Lett 109:267602
44. Allieta M, Scavini M, Spalek LJ et al (2012) Role of intrinsic disorder in the structural phase transition of magnetoelectric $EuTiO_3$. Phys Rev B 85:184107
45. Kim JW, Thompson P, Brown S et al (2013) Emergent superstructural dynamic order due to competing antiferroelectric and antiferrodistortive instabilities in bulk $EuTiO_3$. Phys Rev Lett 110:027201
46. King-Smith RD, Vanderbilt D (1993) Theory of polarization of crystalline solids. Phys Rev B 47:1651–1654
47. Ryan PJ, Kim JW, Birol T et al (2013) Reversible control of magnetic interactions by electric field in a single-phase material. Nat Commun 4:1334
48. Bousquet E, Dawber M, Stucki N et al (2008) Improper ferroelectricity in perovskite oxide artificial superlattices. Nature 452:732–736
49. Benedek NA, Fennie CJ (2011) Hybrid improper ferroelectricity: a mechanism for controllable polarization–magnetization coupling. Phys Rev Lett 106:107204
50. Zanolli Z, Wojdeł JC, Íñiguez J et al (2013) Electric control of the magnetization in $BiFeO_3$–$LaFeO_3$ superlattice. Phys Rev B 88:060102
51. Zhao HJ, Íñiguez J, Ren W et al (2014) Atomistic theory of hybrid improper ferroelectricity in perovskites. Phys Rev B 89:174101
52. Bellaiche L, Íñiguez J (2013) Universal collaborative couplings between oxygen-octahedral rotations and antiferroelectric distortions in perovskites. Phys Rev B 88:014104
53. Mukherjee S, Roy A, Auluck S et al (2013) Room temperature nanoscale ferroelectricity in magnetoelectric $GaFeO_3$ epitaxial thin films. Phys Rev Lett 111:087601
54. Evans DM, Schilling A, Kumar A et al (2013) Magnetic switching of ferroelectric domains at room temperature in multiferroic PZTFT. Nat Commun 4:1534
55. Scott JF (2013) Room-temperature multiferroic magnetoelectrics. NPG Asia Mater 5:e72
56. Zhao HJ, Ren W, Yang Y et al (2014) Near room-temperature multiferroic materials with tunable ferromagnetic and electrical properties. Nat Commun 5:4021
57. Azuma M, Takata K, Saito T et al (2005) Designed ferromagnetic, ferroelectric Bi_2NiMnO_6. J Am Chem Soc. 127:8889–8892
58. Bull CL, McMillan PF (2004) Raman scattering study and electrical properties characterization of elpasolite perovskites $Ln_2(BB')O_6$ (Ln = La, Sm…Gd and B, B′ = Ni Co, Mn). J Solid State Chem 177:2323–2328
59. Rao CNR, Serrao CR (2007) New routes to multiferroics. J Mater Chem 17:4931–4938
60. Cao S, Zhao H, Kang B et al (2014) Temperature induced spin switching in $SmFeO_3$ single crystal. Sci Rep 4:5960